Journal for ImmunoTherapy of Cancer

Durable antitumor response via an oncolytic virus encoding decoy-resistant IL-18

Yan Cheng,[1,2,3] Yuanhui Zhao,[1,2] Yu Liu,[4,5] Yichi Zhang,[6] Dongge Xu,[1,2] Weikang Sun,[1,2] Mengyu Zhang,[1,2,3] Yuqing Miao,[2,3] Susu He,[1,2,3] Yayi Hou ,[1,2] Dwayne Stupack ,[6] Erguang Li [1,2,7]

To cite: Cheng Y, Zhao Y, Liu Y, *et al*. Durable antitumor response via an oncolytic virus encoding decoy-resistant IL-18. *Journal for ImmunoTherapy of Cancer* 2024;**12**:e009716. doi:10.1136/jitc-2024-009716

► Additional supplemental material is published online only. To view, please visit the journal online (https://doi.org/10.1136/jitc-2024-009716).

Accepted 17 October 2024

For numbered affiliations see end of article.

Correspondence to
Dr Dwayne Stupack; dstupack@ucsd.edu

Dr Erguang Li; erguang@nju.edu.cn

ABSTRACT

Background Interleukin-18 (IL-18), or interferon (IFN)-γ-inducing factor, potentiates T helper 1 and natural killer cell activation as well as $CD8^+$ T-cell proliferation. Recombinant IL-18 has displayed limited clinical efficacy in part due to the expression of the decoy receptor, IL-18 binding protein (IL-18BP). A series of IL-18 variants that are devoid of IL-18BP binding, termed DR18 (decoy-resistant IL-18), was developed via directed evolution. We tested DR18 using oncolytic adenovirus (oAd) as a platform for delivery in syngeneic mouse tumor models.

Methods oAd harboring wild-type IL-18 or DR18 (oAdDR18) was constructed by inserting IL-18 mutant into modified oAd backbone with Ad5/3 chimeric fiber. The delivery effect and IFN-γ induction were determined by ELISA. The antitumor efficiency of oAdDR18 was tested in CT26, B16BL6 and 4T1 tumor-bearing mice, or athymic nude mice and compared with recombinant DR18 protein (rDR18). 4T1 lung metastasis model was used to evaluate the antitumor efficiency of local and distant tumors. Antitumor memory and synergistic effect with an anti-programmed cell death protein-1 (PD-1) antibody was evaluated. The phenotypes of the immune cells in tumor microenvironment were analyzed by flow cytometry and immunohistochemistry.

Results Mice received oAdDR18 maintained stable production of IL-18 and IFN-γ compared with those received rDR18. Intratumoral delivery of oAdDR18 significantly reduced tumor growth across several tumor models, but not in the athymic nude mouse model. Mice that had tumor remission showed antitumor memory. The antitumor effect was associated with intratumor infiltration of $CD4^+$ and $CD8^+$ T cells. DR18 delivered by oAd demonstrated long-lasting and enhanced antitumor activities against local and distant tumors compared with that received rDR18 or wild-type IL-18 delivered by oAd (oAdwtIL-18). oAdDR18 treatment also reduced 4T1 lung metastasis. In addition, combination of this virotherapy with immune checkpoint inhibitors (ICIs) like the anti-PD-1 antibody further enhanced the antitumor activity as compared with respective monotherapy.

Conclusions oAdDR18 demonstrates enhanced antitumor activities through the induction of stronger local and system immunities and modulation of the tumor microenvironment compared with those of oAdwtIL-18 and rDR18. A combination of oncolytic virotherapy with cytokine engineering would lead to cytokine-based therapeutics for cancer and other diseases.

WHAT IS ALREADY KNOWN ON THIS TOPIC

⇒ Cytokines are potentially important therapeutics but display short half-lives and toxicity associated with systemic delivery.

WHAT THIS STUDY ADDS

⇒ An oncolytic virotherapy approach that delivers an interleukin (IL)-18 variant (decoy-resistant IL-18) to foster long-lasting and systemic tumor immunity.

HOW THIS STUDY MIGHT AFFECT RESEARCH, PRACTICE OR POLICY

⇒ Cytokine re-engineering combined with virotherapy will broaden cytokine application for targeting therapy.

BACKGROUND

Cytokines produced by a variety of cells act as regulators of innate and adaptive immunity, making them attractive as therapeutics for a variety of immune-related disorders, including cancer.[1 2] "Designer" cytokines with tailored biological activities, can enable precise activation of antitumor immune programs.[3] Interleukin-18 (IL-18), originally identified as interferon (IFN)-gamma-inducing factor, induces IFN-γ secretion, thus enhancing the T helper 1 (Th1) immune response while activating natural killer and cytotoxic T cells.[4]

IL-18 has been proven to enhance immunity against several kinds of tumors, including melanoma and liver cancer since IL-18 directly activates $CD8^+$ T cells and upregulates cytotoxic activity.[5] Recent studies using mouse tumor models have demonstrated the feasibility of using IL-18 as cancer immunotherapy,[6 7] yet clinical trials have not shown the efficacy of this treatment due to rapid pharmacokinetic clearance of rIL-18[8] and the

induction of secreted IL-18-binding protein (IL-18BP), a physiological inhibitor of IL-18, on IL-18 stimulation.[9–11] Abundant expression of IL-18BP is common in cancer. IL-18BP levels are elevated in the circulation of patients with non-small cell lung cancer and increased further by anti-programmed cell death protein-1 (PD-1) or anti-programmed death-ligand 1 treatment.[11] IL-18BP can present at a 20-fold molar excess to that of IL-18 in the serum.[12] In patients treated with rIL-18, serum IL-18BP concentrations increased by 10-fold to 100-fold.[9] Since IL-18BP has an exceptionally high affinity to IL-18 (at approximately 10,000 times higher affinity) compared with that of the target IL-18Rα,[13] the combined molar excess and high affinity represent a major therapeutic barrier, essentially blocking IL-18 activity in vivo.

Bioengineering efforts have yielded new technologies for cytokine engineering.[11 14 15] To improve the effect of IL-18 in vitro and in vivo, one approach which has been used is to introduce amino acid alterations which do not influence target receptor binding or affinity, yet which render IL-18 unable to bind to IL-18BP.[16] Site-directed mutagenesis studies demonstrated that mutants could be isolated which had increased IL-18 to IL-18R binding affinity and enhanced IFN-γ-inducing ability and antitumor activity.[17 18] Directed evolution approaches yielded a series of "decoy-resistant" IL-18s (DR18s) that maintain signaling potential but are impervious to inhibition by IL-18BP.[11] Recombinant DR18 maintained activity in vivo, and elicited potent antitumor effects in mouse tumor models through expanding the pool of stem-like $TCF1^+$ precursor $CD8^+$ T cells.[11 19] Thus, an IL-18 protein that is refractory to control by IL-18BP displays the potent proinflammatory effects of IL-18 on both the innate and adaptive immune system, yielding an antitumor effect.[18 20]

Recombinant cytokines typically exhibit short blood half-lives, and studies from Glaxo Smith Kline demonstrate that rIL-18 is not an exception.[8] Severe side effects associated with dosing can also reduce therapeutic utility.[21–23] For these reasons, we adapted a strategy of sustained, but ultimately self-terminating, local expression via the incorporation of DR18 into an oncolytic viral platform. Broadly, oncolytic viruses selectively cause cancer cell lysis due to their lack of replicative checkpoints. This type of cell death is immunogenic, and oncolytic viruses are considered to be an arm of cancer immunotherapy.[24 25]

Oncolytic adenovirus (oAd) is a commonly used platform for cancer immunotherapy owing to the flexibility of incorporating a genetic payload, thus providing a multimodal strategy to selectively and efficiently target and destroy tumor cells.[24 26 27] Additionally, the *Adenoviridae* are a non-enveloped double-stranded DNA virus that induce robust cell-mediated immune responses, including the production of cytokines. Notably, IL-12, which synergizes with IL-18 for IFN-γ production,[28] is naturally induced by Ad infection,[29] thus skewing tumor-reactive T-cell responses.[30]

We constructed an oAd harboring this decoy-resistant DR18 variant (oAdDR18) and tested its antitumor effect in syngeneic mouse tumor models. We found that intratumoral delivery of oAdDR18 reduced tumor growth on multiple tumor models and improved tumor-infiltrating T lymphocytes (TILs). In addition, oAdDR18 showed local and systemic antitumor effect and lasting antitumor effect. Combining this virotherapy with anti-PD-1 antibody further increased the antitumor activity as compared with virotherapy alone. The work demonstrates that recombinant adenovirus armed with engineered cytokines can be a powerful platform to improve antitumor activities.

MATERIALS AND METHODS

Ethics statement

Protocols for animal experiments were approved by the Animal Experimental Ethics Committee of Nanjing University (Approval no. D2202080) in compliance with the government guidelines for the care and use of laboratory animals.

Cell lines

Mouse and human cell lines of CT26, B16BL6, 4T1, A549, and HEK293 were purchased from ATCC (Manassas, USA) or from Chinese CellBank (Shanghai). The cell lines were cultured under recommended conditions.

Construction and preparation of oncolytic adenoviruses

The viruses were constructed using a 2-plasmid system by homologous recombination in *Escherichia coli* strain BJ5183.[31–33] The backbone plasmid contained a chimeric fiber of Ad5 shaft and Ad3 knob (Ad5/3) for enhanced targeting of tumor cells.[34 35] A shuttle vector, pShuttleE1d24, which contains an E2F promoter for E1A transcription and a designated 24 bp deletion in the CR2 region of E1A for tumor cell-specific replication,[35–37] was constructed. In brief, a complementary DNA for wild-type IL-18 (wtIL-18) (accession Y09278, corresponding to amino acid residues 36–192 of mouse IL-18, NP_032386.1) or the CS2 mutant of DR18 identified by Zhou and colleagues[11] was inserted into the E1 region of pShuttleE1d24. IL-18 lacks a signal peptide, a feature common to the IL-1 family, whose release or maturation requires caspase-1 processing. We used a human albumin signal peptide fused to a mature form of IL-18 for protein secretion. The expression was under the control of human cytomegalovirus (CMV) immediate early enhancer and promoter. The vector was linearized by digestion with Pme I (NEB, R0560V), then transformed into BJ5183 with the backbone vector pAd5/3 to generate pAd-E2F-d24-wtIL-18 or DR18 by homologous recombination. Similarly, a control plasmid (pAd-E2F-d24) without a DNA insert was prepared. To produce the virus, the plasmids were linearized with Pac I (NEB) and transfected into HEK293 cells. The viruses (named oAd, wtIL-18 delivered by oAd (oAdwtIL-18) and oAdDR18, respectively) were confirmed by sequencing analysis for the inserted DNA and by ELISA assay for the secreted protein. The viruses were propagated in HEK293 cells and purified by

ultracentrifugation using a CsCl gradient.[38] Virus concentrations were determined by measuring the absorbance at OD260 with NanoDrop 2000 (Thermo) and converted into viral particles using a coefficient of 1 OD260=1.1×10^{12} vp/mL for conversion.[39]

Preparation of recombinant IL-18 proteins

DNA encoding murine IL-18 (accession Y09278.1) and mutants were synthesized by GenScript (Nanjing) and cloned into pET-21a(+) for expression as C-terminal 6X HIS-tagged proteins in *E. coli* BL21 (DE3) Rosetta strain (Fisher Scientific, #70954–3). For protein expression, freshly prepared bacterial clones were induced with 0.5 mM IPTG for protein expression at 16°C for 20 hours on an orbital shaker (200 rpm). The bacteria were collected by centrifugation and were then resuspended in 30 mL buffer A (1 M NaCl, 10 mM imidazole, 10 mM Tris-HCl, pH 8.0). After sonication for six intervals of 30s-on and 90s-off cycle, the cells were further lysed on ice with 0.5% Triton-100 and 0.1 mg/mL lysozyme (Sigma-Aldrich). The supernatants were collected and incubated with pre-equilibrated 1 mL high-affinity Ni-NTA Resin (GenScript, #L00250) for protein purification by washing with buffer B (1 M NaCl, 10 mM Tris-HCl, pH 8.0) with increased concentrations of imidazole (from 20 mM to 50 mM imidazole). The target protein was eluted with buffer C (1 M NaCl, 200 mM imidazole, 10 mM Tris-HCl, pH 8.0). After analysis by SDS-PAGE, the target protein was pooled and dialyzed against ice-cold phosphate-buffered saline (PBS). After taking concentrations with a Bradford reagent (Bio-Rad, #5000205), the proteins were lyophilized and stored at −80°C.

Preclinical studies

Female C57BL/6 mice, BALB/c and athymic nude mice (6–8 weeks of age) were purchased from SPF (Beijing) Biotechnology and were quarantined for 1 week. Animals were housed under specific pathogen-free conditions. Tumors were grown via a subcutaneous inoculation of CT26 or 4T1 (5×10^5 cells/mouse), or B16BL6 (2×10^5 cells/mouse) cells. Tumor volume was measured and calculated by the formula of length×width^2×0.5. When the tumor volume reached 100 mm^3, mice were randomized into groups. Viral suspensions (1×10^{10} viral particles/dose) in 50 µL PBS were intratumorally injected every other day for a total of five doses. Phosphate-buffered saline alone was considered "mock" treatment. The animals were euthanized when signs of deterioration, acute weight loss, or maximum tumor volume of 2,000 mm^3 were observed. Mice were defined as having achieved complete regression (CR) when the tumor was no longer detected by palpation. To compare the local versus global effect of oAdDR18 and recombinant DR18 protein (rDR18), a bilateral tumor model was used. CT26 cells (5×10^5 cells per injection site) were subcutaneously inoculated into the right and left flanks at the same time. When tumors reached about 100 mm^3, the tumor on the left flank was treated.

For lung metastasis,[40] 4T1 cells were subcutaneously implanted in the rear flank. After tumor establishment (approximately 300 mm^3), 4T1-Luc cells (5×10^5) were injected via the tail vein and luminescence was captured at 2 hours post intravenous injection to assess 4T1-Luc cell distribution. The next day, PBS, rDR18 (0.32 mg/kg), oAdDR18 (1×10^{10} VPs/dose) was injected intratumorally, with dosing repeated on days 3, 5, 7, and 9. On day 10, tumor cell metastasis to the lung was assessed first by in vivo imaging, then mice were harvested and tumor distribution was determined by flow cytometry of digested tissues and by parallel H&E staining of excised lung specimens.

To compare oAdDR18 monotherapy with oAdDR18+anti-PD-1 combination therapy, mice were treated, after establishment of CT26, as follows: For the oAdDR18 monotherapy group, 1×10^{10} VPs/dose were administered on day 1, 3, 5, 7 and 9, for PD-1 monotherapy group, a 100 µg/dose of anti-mouse PD-1 antibody (A2122, Selleck, China)was administered intraperitoneally on day 2, 4, 6, 8, 10, and for combination therapy by intratumoral injections of oAdDR18 or PBS on day 1, 3, 5, 7 and 9 and intraperitoneal injections with anti-PD-1 on day 2, 4, 6, 8, 10.

ELISA and ELISpot assays

IL-18 secretion was measured using an ELISA kit (SinoBiological, KIT50073). Briefly, human A549 or mouse CT26 cells in 96-well plates (1×10^4 cells/well) were infected with oAdDR18 or with control oAd at different virus particles per cell. Culture supernatants were collected at 72 hours post the infection. The concentration of IL-18 in the supernatants was quantitatively determined using a mouse IL-18 ELISA kit with a detection limit of 5.5 pg/mL.

To demonstrate IL-18 production in a tumor setting, mice bearing CT26 tumors (approximately 300 mm^3) were intratumorally injected with rDR18 (0.32 mg/kg), with oAdDR18 (1×10^{10} VPs/mouse, n=3), or with PBS as a control. Mouse blood was collected prior to, and at day 1 and 3 post injection, for measurement of IL-18 and IFN-γ production with Mouse IL-18 and Mouse IFN-γ (KE10001, Proteintech) ELISA kits.

To assess the specific antitumor immune response elicited by oAdDR18, IFN-γ cytokine secretion was detected according to the enzyme-linked immunospot (ELISpot) kit protocol (DAKEWE, DKW22-2000-096). Mouse spleens from PBS, oAd, oAdwtIL-18, or oAdDR18-treated groups were aseptically harvested and isolated. Red blood cells were removed using Red Blood Cell Lysis Solution (Beyotime, Shanghai). The splenocytes (5×10^5 cells/well) were co-cultured with CT26 or 4T1 cells lysate (corresponding with 5×10^4 cells/well, 4T1 cells as a control) at a ratio of 10:1 and incubated for 24 hours at 37°C, 5% CO_2 for in RPMI 1640 medium. Spots were analyzed using the Mabtech IRIS FluoroSpot/ELISpot reader (Mabtech AB).

Table 1 Summary of antibodies used for the study reagent or resource

CD45 monoclonal antibody (30-F11), PE-Cyanine7	eBioscience	cat # 25-0451-82
CD3 monoclonal antibody (17A2), FITC	eBioscience	cat # 11-0032-82
CD8a monoclonal antibody (53–6.7), PE	eBioscience	cat # 12-0081-82
Anti-granzyme B antibody (NGZB), FITC	eBioscience	cat # 11-8898-82
Anti-IFN-γ antibody (XMG1.2), PerCP-Cyanine5.5	eBioscience	cat # 45-7311-80
Anti-mouse CD3ε antibody, PerCP	BioLegend	cat # 100325
Anti-mouse F4/80 antibody, Alexa Fluor 647	BioLegend	cat # 123121
Anti-mouse CD86 antibody, PerCP	BioLegend	cat # 105025
Anti-mouse/human CD11b antibody, FITC	BioLegend	cat # 101205
anti-mouse TCF-1, Alexa Fluor 647	BD Biosciences	cat # 566693

ELISpot, Enzyme-linked Immunosorbent Spot; i.p, Intraperitoneal; i.t, Intratumoral; MOI, Multiplicity of Infection; PBMC, Peripheral Blood Mononuclear Cell.

Flow cytometry

For tumor microenvironment (TME) analysis, tumor or tissue samples were collected and dispersed into single-cell suspensions for flow cytometry analysis. In brief, tumor tissues were cut into small pieces, then resuspended in Dulbecco's Modified Eagle Medium (DMEM) and digested with 200 µg/mL DNase I and 1 mg/mL type I collagenase (Sigma-Aldrich) at 37°C for 30 min. After a brief pipetting, the cells were passed through a cell strainer to make a single-cell suspension.

The cells were stained with appropriate antibodies, while Fixable Viability Dye eFluor 780 (eBioscience, 65086514) was used to distinguish the live cells from the dead cells. Data were acquired on a BD FACSAria III flow cytometer and analyzed using FlowJo software. Antibodies are listed in the key resources table (table 1).

RNA extraction and RT-qPCR

Total RNA from tumor tissues was extracted with Total RNA Extraction Reagent Kit (R401-01, Vazyme) and reversed transcribed with HiScript III RT SuperMix (R323-01, Vazyme) and PCR was performed on an ABI Viia 7 PCR system (Thermo Scientific) using ChamQ SYBR Color qPCR Master reagent mix (Q411, Vazyme). DR18 transgene expression was quantitatively measured by reverse transcription quantitative real-time PCR (RT-qPCR) using the following primers: 5'-GCACCACCGCGGTGATCAG (forward) and 5'-GGTCTGCGGTTCGCTCGCG (reverse). The standard curve was generated using the corresponding DNA as a template for quantification and genome copies/mg tissue was plotted.

Histopathology analysis

Tumor tissues for histopathological analysis were fixed in 4% paraformaldehyde, processed for embedding in paraffin. The samples were sectioned (5 µm thick) and then stained with H&E or immunostained after de-paraffinization and rehydration. For immunohistochemistry, antigen retrieval was performed at 90°C for 20 min according to the manufacturer's suggestions. The antibodies for mouse CD3 (ServiceBio, Wuhan, GB13014-50), CD4 (GB11064-100), CD8 (GB114196-100) were used for immunostaining. After incubation with appropriate secondary antibody, followed by staining with 3,3'-diaminobenzidine (Beyotime) chromogen and hematoxylin counterstain, the samples visualized, and digital images were acquired using an APEXVIEW APX100 system (Olympus). Five randomly selected fields were digitally captured and positively stained cells were quantified using ImageJ software.

Statistical analysis

The statistical significance was determined by one-way analysis of variance tests. A comparison of multiple groups was performed by analysis of least significant difference (LSD) test. *p<0.05; **p<0.01. Kaplan-Meier survival studies used the web Kaplan-Meier plot utility (https://kmplot.com/analysis/) using all patients in the breast cancer and colon cancer curated cohorts.[41] The immunotherapy-treated cohort (all cancers) was stratified to analyze only patients treated with anti-PD-1. Groups were automatically segregated based on the best separation for IL-18/IL-18BP expression.

RESULTS

Characterization of oncolytic virus oAdDR18

A higher ratio of IL-18 to IL-18BP is associated with improved overall survival in both colon and breast cancer (figure 1A,B), supporting the notion that increasing this ratio across patients could result in improved outcome. To this end, recombinant adenoviruses armed with mice wild-type IL-18 and DR18 mutein were constructed by homologous recombination into an adenoviral backbone with Ad5/3 chimeric fiber for improved tumor targeting. The human albumin signal peptide was used for protein secretion. Empty oAd (no payload) were generated as further controls, as illustrated (figure 1C, online supplemental data SI 1).

The ability of oAd to deliver DR18 for in vivo studies was first demonstrated in A549 cells (figure 1D). We detected dose-dependent IL-18 production from

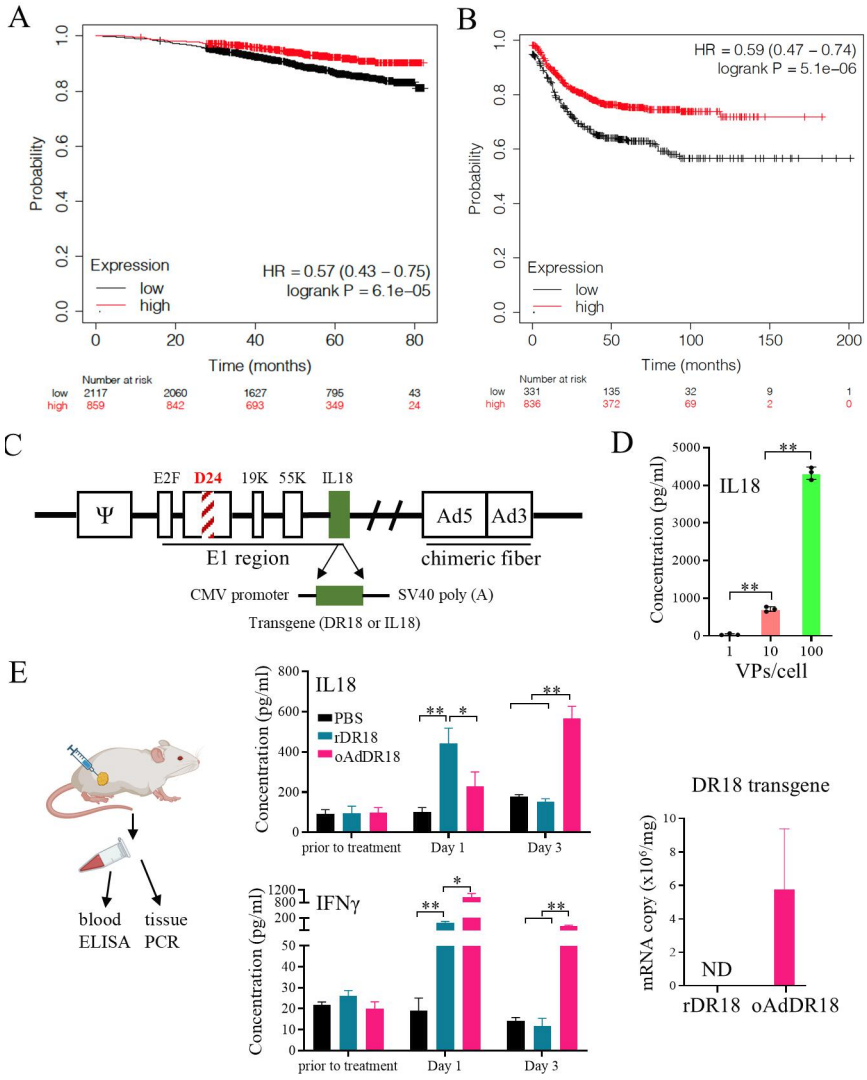

Figure 1 Generation and characterization of oncolytic adenoviruses (A, B) Kaplan-Meier survival curves for breast cancer (A) and colon cancer (B) are shown. Patient cohorts are segregated by the ratio of IL-18 to IL-18BP transcripts (red-high, black-low). The numbers underneath the figures are individuals at each time point. (C) Schematic illustration of oAdDR18. The virus has a 24 bp deletion in the CR2 of the E1A gene, corresponding to the region responsible for Rb protein binding, and is conditionally oncolytic in cells defective in the Rb pathway. The fiber was modified by incorporating the Ad3 knob to the Ad5 shaft and tail for increased tumor targeting (Ad5/3). A complementary DNA for wild-type IL-18 or IL-18BP-binding inactive variant DR18 mCS2 (DR18) was used as transgene for this study. For protein secretion, a signal peptide of human albumin was inserted. (D) DR18 production in oAdDR18-infected A549 cells were determined at 72 hours post infection by quantitative ELISA. Cells in 24-well plates (1×10^5 cells/well) were infected with oAd or oAdDR18 at MOIs as indicated. Data are mean±SD of triplicate samples. (E) IL-18 and IFN-γ production in a tumor setting. After tumor establishment, CT26 xenografts were intratumorally injected with rDR18, oAdDR18, or PBS (n=3). Mouse blood was collected prior to or on days 1 and 3 post injection for measurement of IL-18 and IFN-γ production by ELISA. IL-18 transgene in tumor tissues was further analyzed. DR18, decoy-resistant IL-18; IFN, interferon; IL, interleukin; IL-18BP, IL-18 binding protein; mRNA, messenger RNA; ND, not detectable; oAd, oncolytic adenovirus; oAdDR18, oAd harboring DR18; PBS, phosphate-buffered saline; rDR18, recombinant DR18 protein.

oAdDR18-infected A549 samples. We also tested the capability of IL-18 delivery in vivo by injecting oAdDR18 to established CT26 tumors in mice. Similar to the administration of rDR18, intratumoral injection of oAdDR18 resulted in IL-18 secretion and downstream IFN-γ production (figure 1E). Importantly, the IL-18 transcript was detected in the oAdDR18 group but not the rDR18 groups (figure 1E).

An oncolytic adenovirus armed with DR18 inhibits tumor growth in vivo

To evaluate the impact of oAdDR18 on tumor growth, we next employed several syngeneic tumor models. First, we established tumor transplant models using murine CT26, 4T1 or B16BL6 cells in the respective immunocompetent mice. When the tumors reached approximately 100 mm^3, mice were mock-treated with PBS or treated

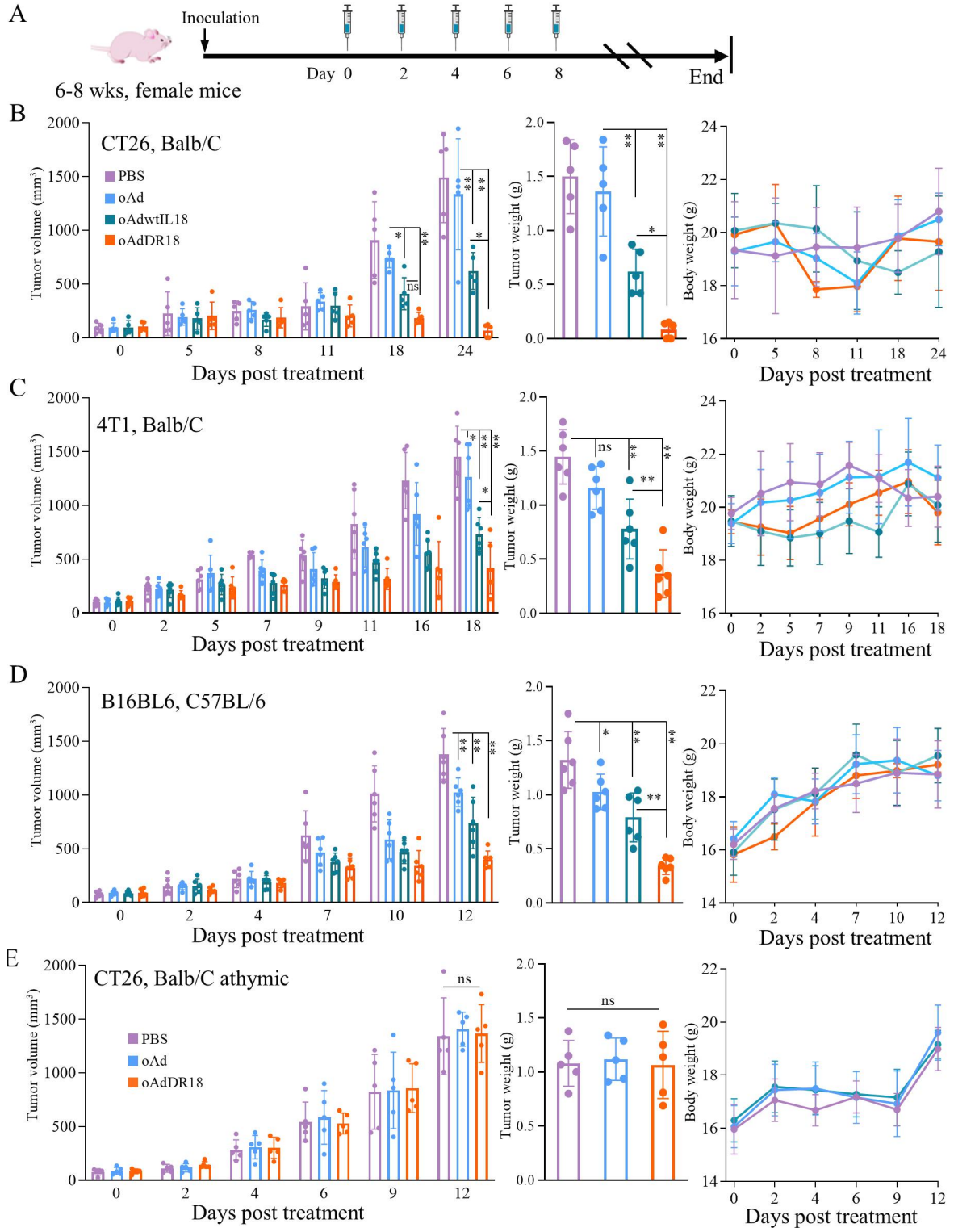

Figure 2 Antitumor effect of oncolytic adenovirus armed with DR18. (A) Illustration of the experimental design. The tumor growth, tumor weight and mouse body weight in (B) CT26 (n=5), (C) 4T1 (n=6), and (D) B16BL6 (n=6) immunocompetent syngeneic tumor models. (E) CT26 tumor growth in athymic nude mice (n=5). DR18, decoy-resistant IL-18; IL, interleukin; oAd, oncolytic adenovirus; oAdDR18, oAd harboring DR18; oAdwtIL-18, wild-type IL-18 delivered by oAd; PBS, phosphate-buffered saline.

with oAd, oAdwtIL-18, oAdDR18 by intratumor injection (figure 2A). As shown, oAdDR18 as well as oAdwtIL-18 demonstrated significant inhibitory activity against tumor growth. In agreement with prior studies documenting the neutralizing effect of IL-18BP, wtIL-18 carried by oAd (oAdwtIL-18) was less effective. In contrast, tumor growth in the oAdDR18-treated group remained relatively slow compared with those in other groups (figure 2B). Notably,

we observed tumor regression in the oAdDR18-treated CT26 tumor model on day 11 and a CR (two out of five mice) on day 24 (figure 2B). In the less immunogenic 4T1 and B16BL6 tumor models, we also observed a more robust antitumor effect by oAdDR18 than in other groups (figure 2C,D). Given the importance of adaptive immunity in tumor restriction, we also repeated the experiment in Balb/C athymic mice. The results showed comparable tumor growth curves (figure 2E), in agreement with past studies showing that T lymphocytes provide a critical contribution to IL-18-mediated antitumor activity.

oAdDR18 treatment increases tumor-infiltrating T lymphocytes

To characterize the frequency and diversity of T cells in the TME, we next examined the accumulation of immune cells. In the CT26 syngeneic tumor model, intratumoral delivery of oAdDR18 resulted in an increase of total T cells ($CD45^+CD3^+$ cells) compared with all other groups (figure 3A, online supplemental data SI 2). The frequency and function of the $CD4^+$ and $CD8^+$ T cells in the production of antitumor immunities induced by oAdDR18 were explored in this study. A significant increase in both $CD8^+$ and $CD4^+$ T cells was observed within the oAdDR18 treated tumors (figure 3B), as evidenced by immunohistochemical staining for total T cells, $CD4^+$ and $CD8^+$ T cells (figure 3C, D, E and F). In addition, tumor-infiltrating inflammatory macrophages (M1-like) increased significantly in mice treated with oAdwtIL-18 and oAdDR18 than with PBS or oAd. However, no difference was observed in the total macrophages across all groups (figure 3G).

During adaptive immune responses, $CD8^+$ and $CD4^+$ T cells are major paracrine sources of IFN-γ. Treatment with oAdDR18 elevated IFN-γ production by $CD4^+$ and $CD8^+$ T cells (figure 3H,I). Cytotoxic T cells are key effectors of antitumor immunity since the cells mediate direct cytolysis of target tumor cells,[42] while some intratumoral $CD4^+$ T cells that express granzymes and perforin can possess cytotoxic programs that directly kill cancer cells.[43] Here, oAdDR18 treatment increased granzyme B-positive $CD8^+$ and $CD4^+$ T cells (figure 3J,K), suggesting that both $CD8^+$ and $CD4^+$ T cells played a significant role in the antitumor immune response. Overall, these results indicate that oAdDR18 treatment was associated with increased tumor infiltration of $CD8^+$, $CD4^+$ T cells and macrophages of antitumor response.

oAdDR18 treatment increases specific cytotoxic activity of T lymphocytes

We investigated whether the increased activation of T cells might reflect a global state of adaptive immunity in the animal. T-cell frequency and activated $CD8^+$ T cells in the blood and spleens from PBS, oAd, oAdwtIL-18, oAdDR18 were examined via flow cytometry. Treatment with any of the oAds—including oAd, oAdwtIL-18 and oAdDR18—increased total T cells and $CD4^+$ T cells in the blood. However, only oAdDR18 treatment was associated with an increase in circulating $CD8^+$ T cells (figure 4A,B). Examining this further using CD69, an early-activation marker expressed by $CD4^+$ and $CD8^+$ T cells, we found $CD8^+CD69^+$ T cells were increased significantly in the oAdDR18 group relative to other groups (figure 4C). This paralleled oAdDR18 mediated increases among the $CD69^+CD8^+$ T cell population in the spleens, although overall, the $CD4^+$ and $CD8^+$ T-cell population exhibited no gross differences across the groups (figure 4D,E).

To assess functionality, we first directly evaluated the activity of CTLs specific to CT26 targets. WT tumor-bearing mice intratumorally injected with PBS, oAd, oAdwtIL-18, oAdDR18 were used as effector cells, and cultured CT26 cells were used as target cells. As shown in figure 4F, the peripheral blood mononuclear cells (PBMCs) from oAdDR18-treated mice, but not from the other groups, showed a marked increase in cytotoxicity versus CT26 cells. Finally, we performed ELISpot assays for IFN-γ release to determine the relative strength of the antitumor response among splenocytes activated by oAdDR18 of the CT26 tumor model. The number of IFN-γ-producing cells was robustly increased in mice treated with oAdDR18 compared with PBS, oAd and oAdwtIL-18 (figure 4G). These global results underscored our initial observations in tissues, reinforcing the notion that intratumoral oAdDR18 elicited a global tumor-specific immune response.

Comparison of local and distant antitumor effect of oAdDR18 and rDR18 by intratumoral injection

The presence of a global response argued that the localized intratumoral injection of oAds could influence distant tumors. To test this, we evaluated a bilateral tumor model in which tumors were implanted in both rear flanks, but only one side was treated (figure 5A). Recombinant DR18 or oAd-based treatment resulted in a local tumor remission relative to PBS controls (figure 5B). However, the only treatment group that exhibited a significant abscopal effect was oAdDR18 (figure 5C,D), as evident by~75% and ~69% inhibition on the treated and distal sides, respectively, relative to PBS controls. This was not associated with changes in mouse body weight (figure 5E). These data support the notion that DR18 delivered by oAd was key to eliciting systemic antitumor activity.

We therefore next tested whether systemic immunity might also limit the growth or establishment of metastases. For this, we again used the metastatic 4T1 cell tumor model, in which subcutaneous and lung seeding were established, then rDR18 or oAdDR18 were administrated intratumorally using PBS as a control and repeated on days 3, 5, 7, and 9. Tumor metastasis to the lungs was first examined by living imaging on day 10, followed by histopathological analysis of the excised lung tissue. Relative to PBS or recombinant protein rDR18-treated mice, which displayed strong tumor signals from the lungs, there was a significantly ($p<0.01$) reduced luciferase signal in oAdDR18-treated mice (figure 5F). Subsequent H&E stains

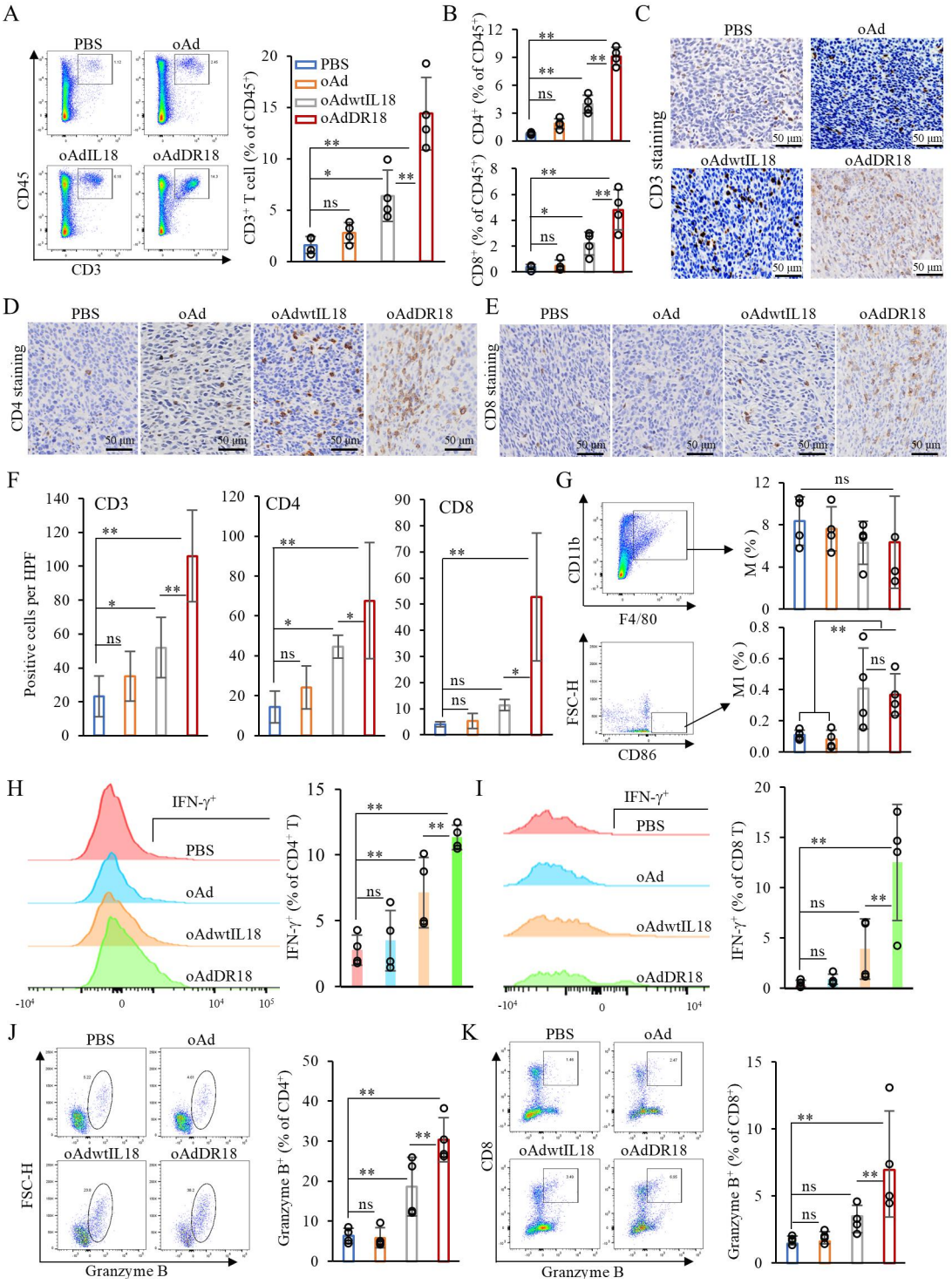

Figure 3 oAdDR18 increases tumor-infiltrating T lymphocytes. (A) Representative flow plots and quantification of the percentage of $CD45^+CD3^+$ T cells in tumor in CT26 tumor model. (B) The percentage of $CD4^+$ T cells and $CD8^+$ T cells of $CD45^+$ cells by flow cytometry. Representative images of immunohistochemical staining for (C) $CD3^+$, (D) $CD4^+$, (E) $CD8^+$, and quantification (F) of the mean number of positively stained cells per high power field (mean±SD). (G) macrophages and M1 in tumor tissues are shown. Representative flow plots and quantification for IFN-γ secretion in $CD4^+$ T cells (H) and in $CD8^+$ T cells (I), granzyme B production of $CD4^+$ T cells (J) and of $CD8^+$ T cells (K). Data are mean±SD (n=4). IFN, interferon; IL, interleukin; oAd, oncolytic adenovirus; oAdDR18, oAd harboring decoy-resistant IL-18; oAdwtIL-18, wild-type IL-18 delivered by oAd; PBS, phosphate-buffered saline.

showed decreased pulmonary colonization and metastatic burden in oAdDR18-treated mice compared with the PBS or rDR18 group (figure 5G). In parallel to the reduced tumor cell burden, higher levels of $CD8^+$ T cells and $CD8^+CD69^+$ T cells were observed in the lungs of oAdDR18-treated mice, relative to PBS

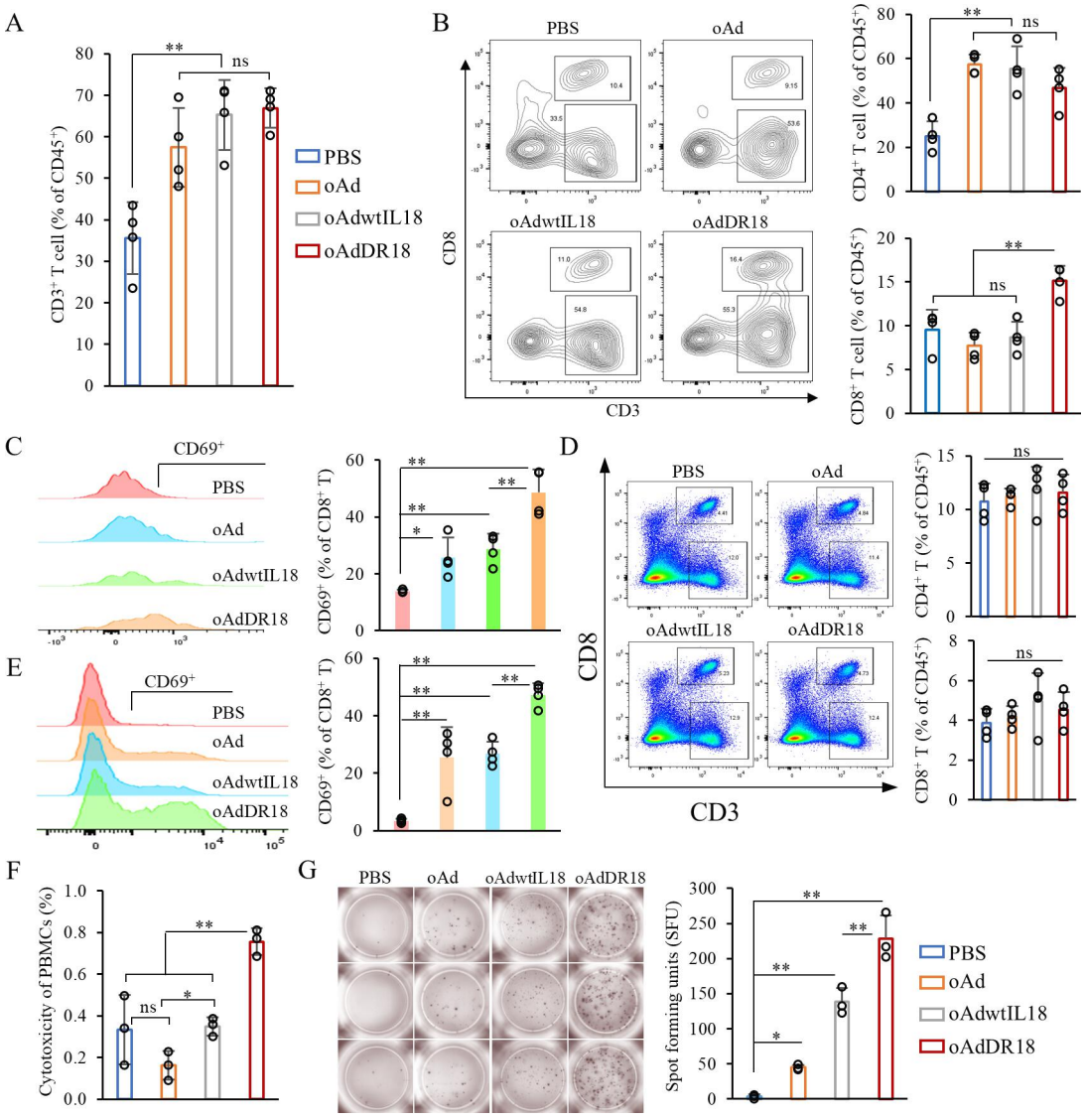

Figure 4 oAdDR18 activated systemic antitumor effect in blood and spleen. (A) Quantification of percentage of $CD45^+CD3^+$ T cells by flow cytometry in blood in CT26 tumor model. (B) Representative flow plots and quantification of $CD4^+$ T cells and $CD8^+$ T cells in the blood. (C) Representative flow plots and quantification of $CD8^+CD69^+$ T cells in the blood. (D) Representative flow plots and quantification of $CD4^+$ T cells and $CD8^+$ T cells in the spleen. (E) Representative flow plots and quantification of $CD8^+CD69^+$ T cells in the spleen. (F) The cytotoxicity of PBMCs. PBMCs from treated tumor-bearing mice were co-cultured with CT26 cells. The ratios between effector PBMCs and target CT26 were at 10:1. Results are expressed as the mean±SD indicated by error bars. (G) ELISpot assay for interferon-γ. The number of spots counted at a concentration of 5×10^5 splenocytes. Each value represents the average±SD of representative of triplicate samples. IL, interleukin; oAd, oncolytic adenovirus; oAdDR18, oAd harboring decoy-resistant IL-18; oAdwtIL-18, wild-type IL-18 delivered by oAd; PBS, phosphate-buffered saline.

or oAdDR18-treated groups (figure 5H,I). Altogether, these observations support the contention that oAdDR18 administrated by intratumoral injection exhibited a systemic antitumor effect against tumor growth and tumor metastasis.

Evaluation of long-term antitumor memory

However, it was not clear if oAdDR18 was capable of eliciting a durable immune response. Since we had observed CR of subcutaneous CT26 tumors (figure 2) among the oAdDR18 treated group, we questioned whether intratumoral administration of oAdDR18 could generate immune memory. Mice cured of CT26 tumors by oAdDR18 were re-challenged 2 months after the last treatment. As controls, 4T1 cells were inoculated in opposite flank. Age-matched mice were used as growth controls. The control mice developed tumors that grew with expected kinetics in treatment-naïve mice subcutaneously inoculated with CT26 or 4T1 cells (figure 6A). In contrast, the cohort of mice that had previously cleared CT26 tumors did not display any occurrence of the secondary inoculated tumors within 22 days of re-challenge (figure 6B–E). This result strongly suggests that oAdDR18 treatment enabled the establishment of long-term antitumor memory.

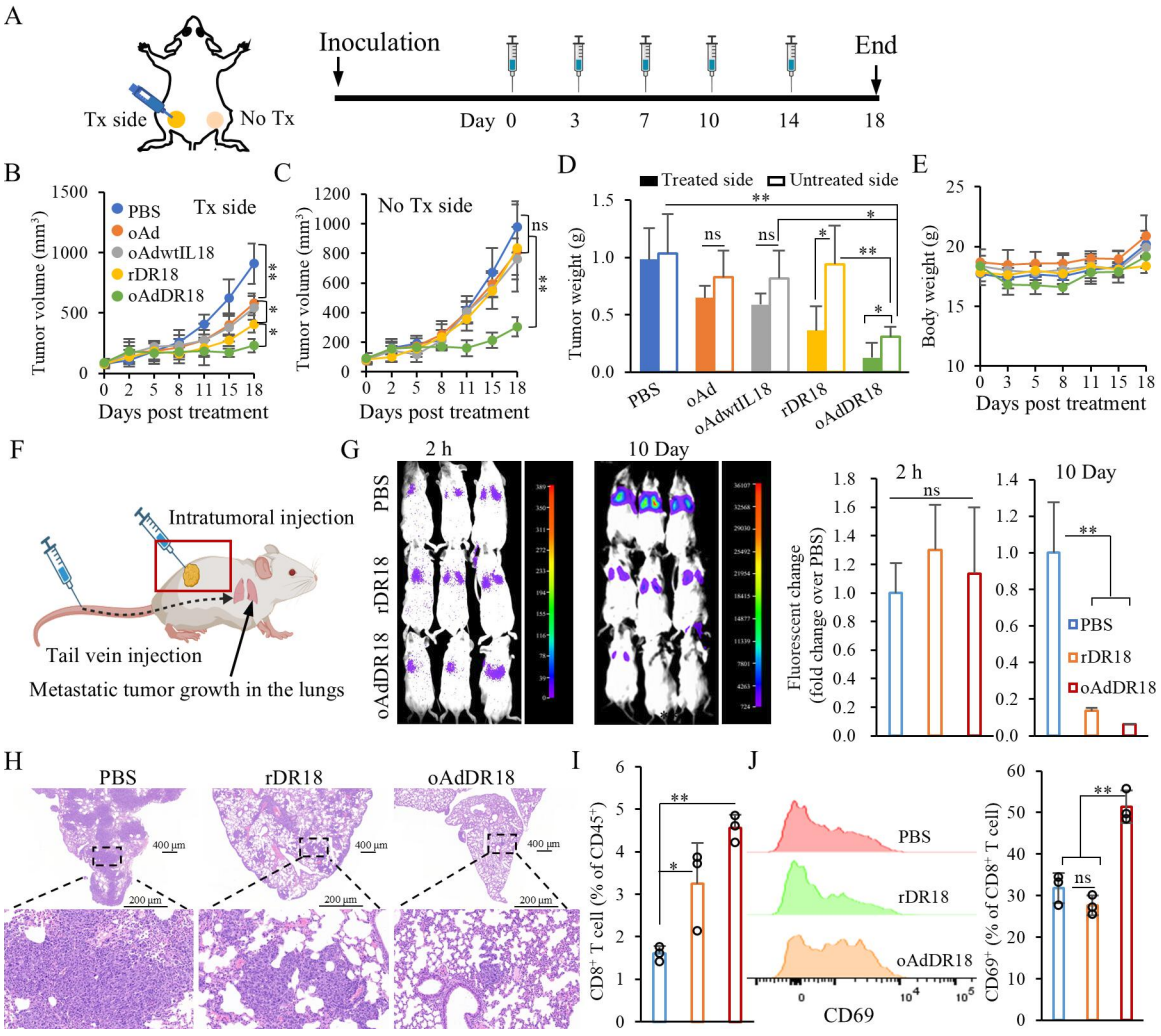

Figure 5 oAdDR18 inhibited non-injected distant tumors and 4T1 tumor metastasis. (A) Diagram illustrating the experimental setups. In the bilateral subcutaneous CT26 model, PBS, oAd, oAdwtIL-18, rDR18 or oAdDR18 was administrated intratumorally on the right tumors twice a week. Tumor growth of treated side (B), untreated side (C), and tumor weight (D) of treated side (solid bar) and untreated side (empty box). (E) Mouse body weight. (F) Diagram of 4T1-Luc lung metastasis model. When the 4T1 tumor inoculated subcutaneously grew up to 300 mm^3, lung metastasis was established by was tail vein injection of 5×10^5 cells 4T1-Luc cells. (G) Live animal bioluminescent images. The images showed entrapped 4T1-Luc cells after 2 hours and 10 days of tail vein injection in the individual group. (H) H&E staining of lung tissue. Representative flow plots and quantification of $CD8^+$ T cells (I), and $CD8^+CD69^+$ T cells (J). IL, interleukin; oAd, oncolytic adenovirus; oAdDR18, oAd harboring decoy-resistant IL-18; oAdwtIL-18, wild-type IL-18 delivered by oAd; PBS, phosphate-buffered saline; rDR18, recombinant decoy-resistant IL-18 protein.

oAdDR18 combined with PD-1 blockade enhances tumor clearance

While oAdDR18 showed remarkable results as a "monotherapy" across multiple tumor models, it did not clear tumors in all cases. We sought to determine if oAdDR18 had a synergistic effect with anti-PD-1, based on recent reports that IFN-γ enhances PD-1 ligand expression, and in turn counteracts immune monitoring and tumor clearance.[44] Indeed, we again observed that among patients treated with PD-1, there was significantly better overall survival associated with high expression of IL-18 (figure 7A). Therefore, we next compared combined oAdDR18 virotherapy and anti-PD-1 immunotherapy in CT26 tumors. Mice received intratumoral injections of oAds or PBS on days 1, 3, 5, 7, and 9 and intraperitoneal injections with anti-PD-1 on days 2, 4, 6, 8, and 10 (figure 7B). The combined therapy eradicated 5/6 tumors in the CT26, more than oAdDR18 or PD-1 monotherapy alone (figure 7C). No weight loss was observed during the experiments (figure 7D).

Although the specific mechanism for the increased efficacy of the combined therapy was not clear, it was interesting that it substantially changed the differentiation program of the $PD\text{-}1^+TCF1^+$ stem-like $CD8^+$ T cells. These were enhanced in the oAdDR18 and oAdDR18+anti-PD-1 group compared with anti-PD-1 monotherapy (figure 7E), suggesting that the immune milieu was indeed further reinforced by dual treatment.

The results collectively demonstrate an immune-mobilizing effect via DR18 delivered by oAd, reducing

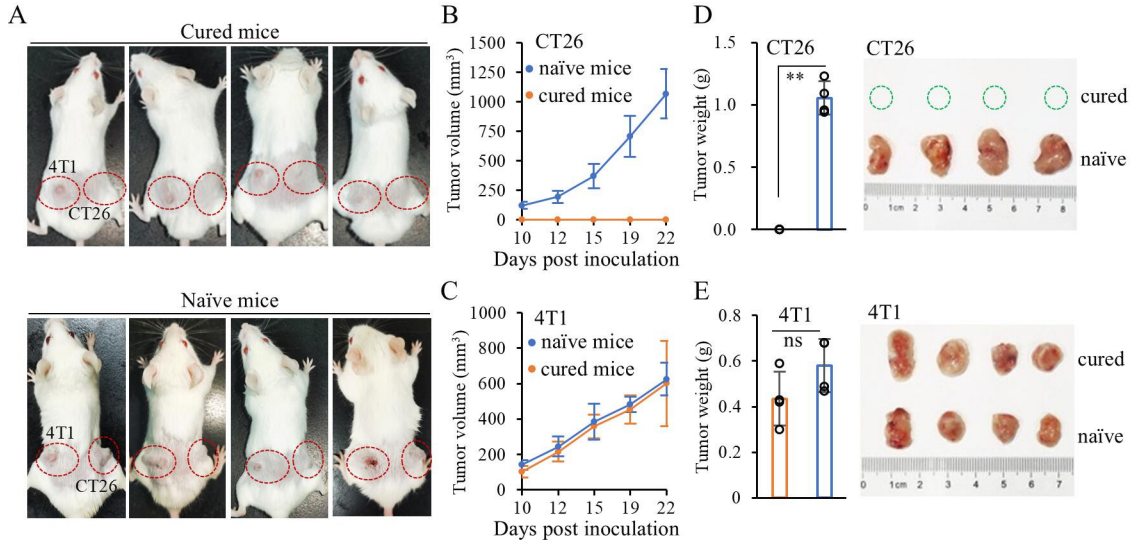

Figure 6 Intratumoral administration of oncolytic adenovirus harboring decoy-resistant interleukin-18induces the establishment of antitumor memory. (A) Mice that achieved complete regression against CT26 tumor and age-matched treatment-naive mice were subcutaneously inoculated with CT26 and 4T1. Images at 10 days after tumor inoculation. (B) CT26 tumor growth. (C) 4T1 tumor growth. (D) CT26 tumor weight and photographs. (E) 4T1 tumor weight and photographs.

tumor growth across multiple tumor models. In comparison to simple recombinant protein delivery to tumors, oAdDR18 treatment improved local and systemic antitumor effects, which were further bolstered by combining with an immune checkpoint inhibitor.

DISCUSSION

Cytokines represent the first modern immunotherapies that have produced durable immune response in patients with advanced cancers. More widespread use of recombinant cytokines is functionally limited by short half-lives following systemic delivery, and due to toxicities associated with acutely extreme elevations in cytokine concentration.[15 45] In this regard, a lower but constant level of cytokine production may offer a more physiologic approach to immunotherapy.

Cytokine activity may also depend on context, and can have varying effect depending on whether it is establishing versus enhancing an immune response. In the case of IL-18, it is clear that lower levels of IL-18 versus IL-18BP transcripts are associated with disease outcome. While it was perhaps not surprizing for DR18 to bolster as immune response in these studies, the profound level of response, including complete responses, was completely unexpected. IL-18 displays pleiotropic actions, depending on the local cytokine milieu. It acts on Th1 cells, macrophages, natural killer (NK) cells, natural killer T (NKT) cells, B cells, dendritic cells, and even nonpolarized T cells to produce IFN-γ in the presence of IL-12. In the absence of IL-12, IL-18 with IL-2 induces type 2 T helper cytokines from NK cells or NKT cells with a $CD4^+$ phenotype, and even committed Th1 cells,[7 46] which can be detrimental to antitumor immunity.

A limit and advantage of adenoviral therapy is the profound immune response elicited by the viral components themselves. Adenoviral vectors are well known to induce host immune response, including the production of cytokines like I-L1β, IL-6, IL-8, IL-12, IFN-γ, IFN-α, TNF-α, and chemokines like CCL2, CCL3, and CXCL10.[29] This serves as an immune adjuvant role in promoting tumor clearance, since the tumoricidal activity of the oAd alone was of limited benefit in controlling tumor growth. oAdDR18 resulted in the robust tumor inhibition over its wild-type counterpart or rDR18 in CT26, B16BL6 and 4T1 tumors. Compared with recombinant DR18, intratumoral injection of oAdDR18 showed long-term and systemic antitumor effect in syngeneic mouse models. Thus, the ability to package a decoy-resistant IL-18 was similarly critical in boosting the antitumor effect, with the addition of a checkpoint inhibitor (anti-PD-1) showing the greatest potential for tumor control.

The use of intratumoral injection was essential to this study, due to the dependence of oAd on the proliferation of dysregulated cells (such as tumors). However, local tumor injection impacted both distant bilateral tumors and small metastases, thus reinforcing the notion that not all tumors need to be injected to have positive outcomes. The signal from a local injection acted globally and durably, since rechallenge with tumor cells (CT26) did not result in de novo tumor formation among mice that had previously cleared those tumors. Consistent with this, improved $CD4^+$ and $CD8^+$ T-cell antitumor responses including frequency and cytotoxicity, as demonstrated by immune cell analysis and immunohistochemistry. Both the global and durable aspects are key components for therapies that will have clinical utility.

In this regard, adenoviral vectors are extensively studied in experimental and clinical models as agents for gene therapy. As we observed, they potently deliver and express key genes of interest, yet are self-limiting. Their use in oncology appears quite safe, and their immune effects are well understood. A Th1 dominant antiviral immune response occurs 5–7 days following transduction.[47] This is

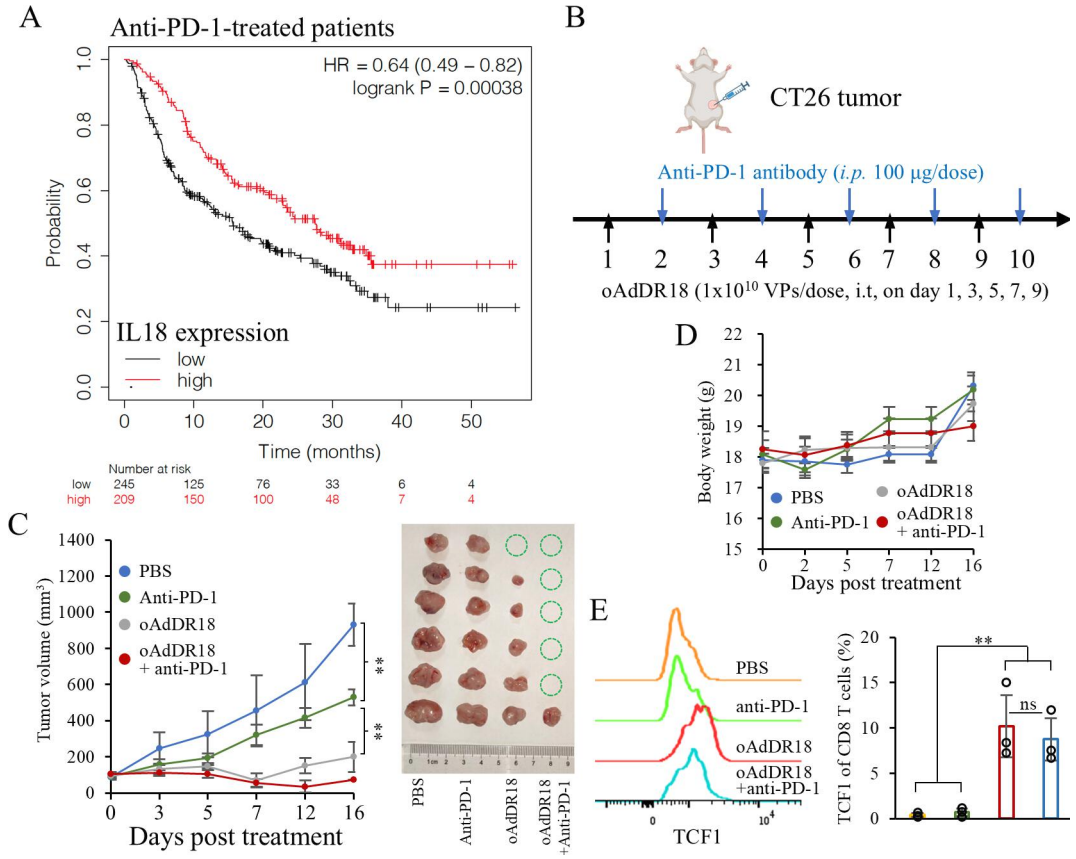

Figure 7 Combination therapy of oAdDR18 and anti-PD-1 antibody (A) Kaplan-Meier survival curve. Immunotherapy-treated cohort (all cancers) was stratified to analyze only patients treated with anti-PD-1 breast cancer. The numbers underneath the figures are individuals at each time point. (B) Diagram illustrating the experimental setups. Balb/c mice were subcutaneously (s.c.) engrafted with 5×10^5 CT26 cells. When the tumor grew up to approximately 100 mm^3, mice were treated with PBS or oAdDR18 (i.t), or anti-PD-1 or a combination of oAdDR18 (i.t) + anti-PD-1 antibody (i.p). (C) Tumor growth. (D) The photographs of collected tumors. (E) Body weight. (F) The representative flow plots and quantification of $TCF1^+$ of $CD8^+$ T cells by flow cytometry. Mice were inoculated with CT26 cells and were treated on day 1 and day 3 with PBS, oAdDR18, or anti-PD-1 on days 2 and 4. Tumor-bearing mice were sacrificed 3 days after the last anti-PD-1 treatment and tumor tissues were removed and used for flow cytometry analysis. IL, interleukin; oAdDR18, oncolytic adenovirus harboring decoy-resistant IL-18; PBS, phosphate-buffered saline; PD-1, programmed cell death protein-1.

partly due to adenovirus-associated-IL-12 expression. IL-12 acts as a cytokine that induces Th1 polarization and synergistically acts with IL-18 (or DR18) to enhance the cytotoxic functions of TILs.[6 48] oAd co-expressing IL-12 and "wt" IL-18 improves tumor-specific immunity via differentiation of T cells.[49] However, oAd armed with decoy-resistant IL-18 ligand appears well-suited to shape the TME for enhanced anti-tumor immunity, and is complemented by anti-PD-1. These data support the further exploration of oAd as a potent, self-limiting approach to immunotherapy in cancer together with complementary modulators of immune function, including vaccines or other checkpoint inhibitors.

Cytokines have pivotal roles in immunity and have been demonstrated as therapeutics for a variety of immune-related disorders. However, the widespread clinical use of cytokines has been limited by their short half-lives and defects for systemic application. Innovations in bioengineering and in the evolution of enzymes have yielded new technologies for cytokine engineering and aided in advancing our knowledge of cytokine biology. Thus, a combination of oncolytic virotherapy with cytokine engineering would lead to cytokine-based therapeutics for cancer and other diseases.

Author affiliations
[1]State Key Laboratory of Biotechnology, Medical School, Nanjing University, Nanjing, China
[2]Jiangsu Key Laboratory of Molecular Medicine, Medical School, Nanjing University, Nanjing, China
[3]The No. 1 People's Hospital of Yancheng City, Nanjing University Medical School, Yancheng, China
[4]Shanghai No. 10 Peoples Hospital, Shanghai, China
[5]Cancer Research Center, Shanghai No. 10 People's Hospital, Shanghai, China
[6]Moores Cancer Center, University of California San Diego, La Jolla, California, USA
[7]Institute of Medical Virology, Affiliated Gulou Hospital of Nanjing University Medical School, Nanjing, China

Present affiliations The present affiliation of Susu He is: Dartmouth Geisel School of Medicine, Hanover, New Hampshire, USA.

X Dwayne Stupack @dwaynestupack

Acknowledgements The authors would like to thank staff members from Jiangsu Key Laboratory of Molecular Medicine for technical support.

Contributors Concept and design, EL, YC, DS conceived the study; experiments, EL, YC and SH designed and carried out the experiments, and performed the analyses with contributions from YZhao, YL, DX, WS, MZ, and YZhang; YC contributed to data analyses and designed the figures with input from all authors. EL, SH, YH, YM and DS acquired funding; draft writing, EL, YC and DS, editing, EL, YC, YH and DS. All authors have approved the current submission: EL is the Guarantor.

Funding The work was supported by grants from National Key R&D Program of China (2023YFC2308200 to EL and YH), Curebound (2023 Discovery Award to DGS), NSFC (81871636 to EL), Jiangsu Natural Science Foundation (BK20200316 to SH), Yancheng People's First Hospital for collaboration in research (to EL and YM), and grant from State Key Laboratory of Pharmaceutical Biotechnology of Nanjing University. YC and WS were recipients of Jiangsu Graduate Student Innovation Program

Competing interests No, there are no competing interests.

Patient consent for publication Not applicable.

Ethics approval Not applicable.

Provenance and peer review Not commissioned; externally peer reviewed.

Data availability statement Data are available upon reasonable request. Not Applicable.

ORCID iDs
Yayi Hou http://orcid.org/0000-0002-1152-9132
Dwayne Stupack http://orcid.org/0000-0003-4396-5745
Erguang Li http://orcid.org/0000-0002-3065-1336

REFERENCES

1 Saxton RA, Glassman CR, Garcia KC. Emerging principles of cytokine pharmacology and therapeutics. *Nat Rev Drug Discov* 2023;22:21–37.
2 Propper DJ, Balkwill FR. Harnessing cytokines and chemokines for cancer therapy. *Nat Rev Clin Oncol* 2022;19:237–53.
3 Spangler JB, Moraga I, Mendoza JL, *et al*. Insights into cytokine-receptor interactions from cytokine engineering. *Annu Rev Immunol* 2015;33:139–67.
4 Dinarello CA. IL-18: A TH1-inducing, proinflammatory cytokine and new member of the IL-1 family. *J Allergy Clin Immunol* 1999;103:11–24.
5 Kaplanski G. Interleukin-18: Biological properties and role in disease pathogenesis. *Immunol Rev* 2018;281:138–53.
6 Chirathaworn C, Poovorawan Y. *IL-18 in Regulation of Antitumor Immune Response and Clinical Application.* New York, NY: Springer,
7 Ihim SA, Abubakar SD, Zian Z, *et al*. Interleukin-18 cytokine in immunity, inflammation, and autoimmunity: Biological role in induction, regulation, and treatment. *Front Immunol* 2022;13:919973.
8 Robertson MJ, Kline J, Struemper H, *et al*. A dose-escalation study of recombinant human interleukin-18 in combination with rituximab in patients with non-Hodgkin lymphoma. *J Immunother* 2013;36:331–41.
9 Robertson MJ, Mier JW, Logan T, *et al*. Clinical and biological effects of recombinant human interleukin-18 administered by intravenous infusion to patients with advanced cancer. *Clin Cancer Res* 2006;12:4265–73.
10 Tarhini AA, Millward M, Mainwaring P, *et al*. A phase 2, randomized study of SB-485232, rhIL-18, in patients with previously untreated metastatic melanoma. *Cancer* 2009;115:859–68.
11 Zhou T, Damsky W, Weizman O-E, *et al*. IL-18BP is a secreted immune checkpoint and barrier to IL-18 immunotherapy. *Nature New Biol* 2020;583:609–14.
12 Novick D, Schwartsburd B, Pinkus R, *et al*. A novel IL-18BP ELISA shows elevated serum IL-18BP in sepsis and extensive decrease of free IL-18. *Cytokine* 2001;14:334–42.
13 Dinarello CA, Novick D, Kim S, *et al*. Interleukin-18 and IL-18 binding protein. *Front Immunol* 2013;4:289.
14 Kim SH, Azam T, Yoon DY, *et al*. Site-specific mutations in the mature form of human IL-18 with enhanced biological activity and decreased neutralization by IL-18 binding protein. *Proc Natl Acad Sci U S A* 2001;98:3304–9.
15 Deckers J, Anbergen T, Hokke AM, *et al*. Engineering cytokine therapeutics. *Nat Rev Bioeng* 2023;1:286–303.
16 Sun R, Gao DS, Shoush J, *et al*. The IL-1 family in tumorigenesis and antitumor immunity. *Semin Cancer Biol* 2022;86:280–95.
17 Swencki-Underwood B, Cunningham MR, Heavner GA, *et al*. Engineering human IL-18 with increased bioactivity and bioavailability. *Cytokine* 2006;34:114–24.
18 Saetang J, Puseenam A, Roongsawang N, *et al*. Immunologic Function and Molecular Insight of Recombinant Interleukin-18. *PLoS One* 2016;11:e0160321.
19 Hu B, Ren J, Luo Y, *et al*. Augmentation of Antitumor Immunity by Human and Mouse CAR T Cells Secreting IL-18. *Cell Rep* 2017;20:3025–33.
20 Dixon KO, Kuchroo VK. IL-18: throwing off the shackles to boost anti-tumor immunity. *Cell Res* 2020;30:831–2.
21 Waldmann TA. Cytokines in Cancer Immunotherapy. *Cold Spring Harb Perspect Biol* 2018;10:a028472.
22 Leonard WJ, Lin JX. Strategies to therapeutically modulate cytokine action. *Nat Rev Drug Discov* 2023;22:827–54.
23 Briukhovetska D, Dörr J, Endres S, *et al*. Interleukins in cancer: from biology to therapy. *Nat Rev Cancer* 2021;21:481–99.
24 Twumasi-Boateng K, Pettigrew JL, Kwok YYE, *et al*. Oncolytic viruses as engineering platforms for combination immunotherapy. *Nat Rev Cancer* 2018;18:419–32.
25 Tian Y, Xie D, Yang L. Engineering strategies to enhance oncolytic viruses in cancer immunotherapy. *Signal Transduct Target Ther* 2022;7:117.
26 Harrington K, Freeman DJ, Kelly B, *et al*. Optimizing oncolytic virotherapy in cancer treatment. *Nat Rev Drug Discov* 2019;18:689–706.
27 Shalhout SZ, Miller DM, Emerick KS, *et al*. Therapy with oncolytic viruses: progress and challenges. *Nat Rev Clin Oncol* 2023;20:160–77.
28 Yoshimoto T, Takeda K, Tanaka T, *et al*. IL-12 up-regulates IL-18 receptor expression on T cells, Th1 cells, and B cells: synergism with IL-18 for IFN-gamma production. *J Immunol* 1998;161:3400–7.
29 Atasheva S, Shayakhmetov DM. Cytokine Responses to Adenovirus and Adenovirus Vectors. *Viruses* 2022;14:888.
30 Li Q, Carr AL, Donald EJ, *et al*. Synergistic Effects of IL-12 and IL-18 in Skewing Tumor-Reactive T-Cell Responses Towards a Type 1 Pattern. *Cancer Res* 2005;65:1063–70.
31 Uil TG, Seki T, Dmitriev I, *et al*. Generation of an adenoviral vector containing an addition of a heterologous ligand to the serotype 3 fiber knob. *Cancer Gene Ther* 2003;10:121–4.
32 Dmitriev I, Krasnykh V, Miller CR, *et al*. An adenovirus vector with genetically modified fibers demonstrates expanded tropism via utilization of a coxsackievirus and adenovirus receptor-independent cell entry mechanism. *J Virol* 1998;72:9706–13.
33 He TC, Zhou S, da Costa LT, *et al*. A simplified system for generating recombinant adenoviruses. *Proc Natl Acad Sci U S A* 1998;95:2509–14.
34 Kanerva A, Wang M, Bauerschmitz GJ, *et al*. Gene transfer to ovarian cancer versus normal tissues with fiber-modified adenoviruses. *Mol Ther* 2002;5:695–704.
35 Fueyo J, Gomez-Manzano C, Alemany R, *et al*. A mutant oncolytic adenovirus targeting the Rb pathway produces anti-glioma effect in vivo. *Oncogene* 2000;19:2–12.
36 Helin K, Lees JA, Vidal M, *et al*. A cDNA encoding a pRB-binding protein with properties of the transcription factor E2F. *Cell* 1992;70:337–50.
37 Mantwill K, Klein FG, Wang D, *et al*. Concepts in Oncolytic Adenovirus Therapy. *Int J Mol Sci* 2021;22:10522.
38 Luo J, Deng Z-L, Luo X, *et al*. A protocol for rapid generation of recombinant adenoviruses using the AdEasy system. *Nat Protoc* 2007;2:1236–47.
39 Berkowitz SA. Determining the concentration and the absorptivity factor at 260 nm in sodium dodecyl sulfate of the adenovirus reference material using analytical ultracentrifugation. *Anal Biochem* 2008;380:152–4.

40 Secondini C, Coquoz O, Spagnuolo L, *et al*. Arginase inhibition suppresses lung metastasis in the 4T1 breast cancer model independently of the immunomodulatory and anti-metastatic effects of VEGFR-2 blockade. *Oncoimmunology* 2017;6:e1316437.
41 Győrffy B. Transcriptome-level discovery of survival-associated biomarkers and therapy targets in non-small-cell lung cancer. *Br J Pharmacol* 2024;181:362–74.
42 Mellman I, Coukos G, Dranoff G. Cancer immunotherapy comes of age. *Nature New Biol* 2011;480:480–9.
43 Oh DY, Fong L. Cytotoxic CD4+ T cells in cancer: Expanding the immune effector toolbox. *Immunity* 2021;54:2701–11.
44 Mandai M, Hamanishi J, Abiko K, *et al*. Dual Faces of IFNγ in Cancer Progression: A Role of PD-L1 Induction in the Determination of Pro- and Antitumor Immunity. *Clin Cancer Res* 2016;22:2329–34.
45 Szefel J, Danielak A, Kruszewski WJ. Metabolic pathways of L-arginine and therapeutic consequences in tumors. *Adv Med Sci* 2019;64:104–10.
46 Saravia J, Chapman NM, Chi H. Helper T cell differentiation. *Cell Mol Immunol* 2019;16:634–43.
47 Yang Y, Ertl HC, Wilson JM. MHC class I-restricted cytotoxic T lymphocytes to viral antigens destroy hepatocytes in mice infected with E1-deleted recombinant adenoviruses. *Immunity* 1994;1:433–42.
48 Z-f C, R Z, B XIA, *et al*. Interleukin-18 and -12 synergistically enhance cytotoxic functions of tumor-infiltrating lymphocytes. *Chin Med J* 2012;125:4245–8.
49 Choi I-K, Lee J-S, Zhang S-N, *et al*. Oncolytic adenovirus co-expressing IL-12 and IL-18 improves tumor-specific immunity via differentiation of T cells expressing IL-12Rβ2 or IL-18Rα. *Gene Ther* 2011;18:898–909.